J. Phys. D: Appl. Phys. 26 (1993) 2219–2225. Printed in the UK

Roughness effect on friction for multi-asperity contact between surfaces

I J Ford

Theoretical Studies Department, AEA Technology, B424.4, Harwell Laboratory, Didcot, Oxon OX11 0RA, UK

Received 5 July 1993, in final form 25 August 1993

Abstract. A combined adhesion–roughness model of friction, originally developed for contact between a narrow slider and a single asperity, is applied to the case of multiple asperity contact between rough surfaces. An analytical model, based on the Greenwood–Williamson model of asperity contact, leads to a simple roughness-dependent expression for the friction coefficient. For elastic deformation at each contact point, the contribution due to roughness is half that suggested by the single asperity analysis. When contact is largely plastic, the roughness contribution is half the elastic contribution. The reduction is mainly due to cancellation when forces at the various asperities in contact are summed. Example calculations are performed for rough diamond surfaces, using numerically generated surfaces.

1. Introduction

The first attempt to relate friction to the roughness of a surface is associated with Coulomb [1]. Friction was taken to be the force required to move the point of contact between two surfaces up the incline of an asperity against the applied load. However, it was realized soon afterwards [2] that the energy expended in doing so was returned during the descent down the other side of the asperity, so that the frictional force was on average zero. However, these ideas were developed later by Tabor who introduced an adhesive frictional force at the contact, which removed the symmetry between ascent and descent [3]. The energy required to ascend an asperity is then not all returned during the descent, yielding a non-zero coefficient of friction, with a particular dependence on roughness. This mechanism was extended by Seal [4] to allow for sliding over a two-dimensional surface.

However, in both Tabor's and Seal's analyses, contact between a narrow slider and the surface is considered, such that the slider encounters one asperity at a time. A more realistic contact situation between two rough surfaces should involve simultaneous interaction at many asperities. In this paper such a model is developed, and the results of the analysis compared with the single-asperity model.

In the next section the single-asperity model is reviewed, and then an analytical development of multi-asperity contact is described, based on the Greenwood–Williamson model [5]. In section 3 numerical calculations of friction between two rough diamond surfaces are presented, as a check on the results of the analytical model. Section 4 contains a discussion of the models and conclusions, together with some comments on the interpretation of experimental friction coefficients [6] for diamond films.

2. The Tabor model

2.1. One asperity

The Tabor mechanism was developed originally [3] for the simple situation where a narrow slider passes over a single pointed asperity, as shown in figure 1. The local normal at the contact point is inclined at an angle θ to the vertical, and the surface is taken to be one-dimensional. The angle θ will be referred to as the contact angle. The local friction force $\mathcal{F}$ resisting motion from left to right in figure 1 is related to the local normal force W by $\mathcal{F} = \mu_0 W$ where μ_0 is the underlying friction

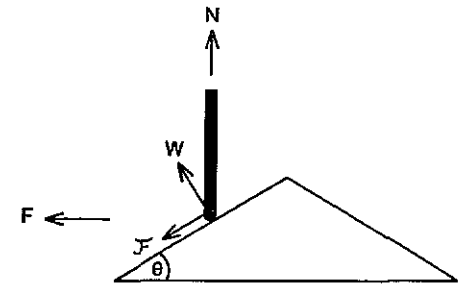

Figure 1. Situation considered by the Tabor model. A narrow slider moves over a pointed symmetrical asperity with angle of climb θ. Local reaction and friction contribute towards overall vertical and horizontal forces.

0022-3727/93/122219+07$07.50 © 1993 IOP Publishing Ltd

coefficient, due, it is assumed, to adhesion. The vertical and horizontal components of force acting on the slider are given by

$$N = W\cos\theta - \mathcal{F}\sin\theta \tag{1}$$

and

$$F = W\sin\theta + \mathcal{F}\cos\theta \tag{2}$$

respectively, and the effective friction coefficient for the ascent of the asperity is therefore

$$\mu(\theta) = \frac{F}{N} = \frac{\mu_0 + \tan\theta}{1 - \mu_0\tan\theta}. \tag{3}$$

When the slider passes individually over many symmetric asperities, each with an angle of climb θ, the friction coefficient fluctuates as the slider ascends and then descends. Its average value is, however,

$$\mu = \frac{1}{2}(\mu(\theta) + \mu(-\theta)) = \frac{\mu_0(1 + \tan^2\theta)}{1 - \mu_0^2\tan^2\theta}. \tag{4}$$

The roughness of a surface is determined by both the angle θ and the surface correlation lengths: for constant values of the latter, roughness increases with increasing θ [8]. Equation (4) represents, therefore, a roughness-dependent friction coefficient. This model has recently been used to account for the observed roughness dependence of the friction coefficient of diamond films, where θ for individual asperities can be as high as 70–80° [6].

The restriction to one-dimensional surfaces has been removed by further development of the model [4]. For two-dimensional surfaces, motion of the contact point around the shoulders of asperities has to be taken into account. However, the friction coefficient retains a dependence on the angle of climb over the asperities, and hence on the roughness of the surface.

2.2. Many asperities

The analysis presented above applies to contact between a point slider moving over a single asperity or to contact between periodic corrugated surfaces with every point of contact identical. A more realistic situation involves two random two-dimensional rough surfaces which make contact at many asperities. We now present an analysis based on the Greenwood–Williamson model of rough surface contact [5], which takes into account the inclination at each contact point.

Figure 2 illustrates the situation considered in two equivalent ways: in (*a*) the real geometry of the contacting surfaces (represented in one dimension) is shown, and in (*b*) contact of the effective rough surface with a rigid flat surface. The effective rough surface is just the gap between the two surfaces, and the material properties are a combination of those of the two real

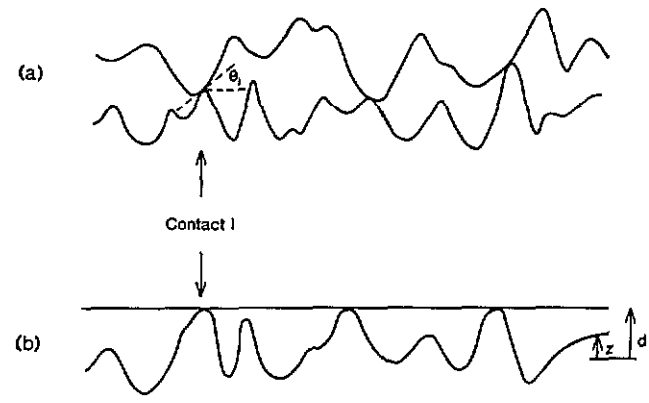

Figure 2. Contact between two one-dimensional rough surfaces. The real geometry in (*a*) can be treated using an effective rough surface in contact with a flat in (*b*). The real contact angle θ_i alters the apparent indentation at the ith contact point in (*b*). Surfaces shown just touching.

surfaces. This is a standard construction in contact mechanics [7].

However, it must be remembered that each contact shown in figure 2(*b*) is not in fact normal but is characterized by a non-zero inclination angle: this is taken into account in the following development. Figures 2(*a*) and (*b*) are merely topologically equivalent. It would perhaps be possible to develop the model using the contact of two rough surfaces as in figure 2(*a*), but the rough-on-flat surface approach has been developed here because it corresponds more closely to the numerical work to be described in section 3.

Consider the rigid flat to be horizontal. The height of the ith asperity of the effective rough surface relative to its mean plane is z_i. In the usual Greenwood–Williamson development, the indentation at the ith asperity in figure 2(*b*) would normally be the interference $(z_i - d)$ between the rough surface and the rigid flat at height d above the mean plane. However, since the ith contact is inclined to the vertical at an angle θ_i, the actual indentation normal to the local tangent plane at asperity i is

$$\delta_i = (z_i - d)\cos\theta_i. \tag{5}$$

This means that, for a given plane separation d in figure 2(*b*), the real indentation at a contact decreases as the angle of contact increases.

The contact angle θ is the angle between the horizontal plane and the line of steepest ascent on the surface at the point of contact. The geometry at the contact is illustrated in figure 3. The direction of sliding is, in general, not along the line of steepest ascent, but rather at a resolved angle α to that direction, so that the real angle of ascent θ' is less than θ. Simple geometry yields $\tan\theta' = \cos\alpha\tan\theta$.

We now drop the suffix i and write the (normalized) distribution of heights z of asperities on the effective surface as $\phi(z)$. Each contact is characterized by a contact angle θ, and for a chosen direction of sliding, an angle α, with distributions $\psi(\theta)$ and $\zeta(\alpha)$, respectively. It is assumed that θ and α are not correlated with each other, nor with the asperity height.

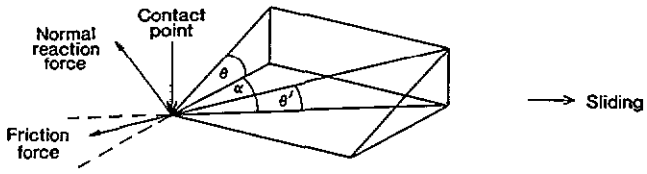

Figure 3. The geometry of contact on the flank of an asperity on a two-dimensional surface The maximum inclination angle at the point of contact is θ, and α is the angle between the direction of steepest slope and the direction of sliding. The actual angle of ascent during sliding is θ'.

The area of contact at the ith asperity of the effective rough surface depends on the local indentation δ_i, and is written

$$A_i = f(\delta_i). \tag{6}$$

The local friction force at each asperity is $\mathcal{F}_i = A_i s$, where s is the shear stress required to break the adhesive bonds at the contact. The local normal reaction force is

$$W_i = g(\delta_i) \tag{7}$$

with $f(\delta)$ and $g(\delta)$ particular functions of indentation distance δ.

The resolution of forces at each asperity is carried out in a manner analogous to equations (1) and (2) above, but extended to a two-dimensional surface. The total vertical force due to contact between the effective surface and the rigid flat is given by

$$N = \int_d^\infty \{g((z-d)\cos\theta)\cos\theta - sf((z-d)\cos\theta)\sin\theta'\} \times \phi(z)\psi(\theta)\zeta(\alpha)\,dz\,d\theta\,d\alpha. \tag{8}$$

The horizontal force opposing the sliding from left to right is

$$F = \int_d^\infty \{g((z-d)\cos\theta)\sin\theta\cos\alpha + sf((z-d)\cos\theta)\cos\theta'\} \times \phi(z)\psi(\theta)\zeta(\alpha)\,dz\,d\theta\,d\alpha. \tag{9}$$

The angular integrals are taken over the full available range, while the integrals over z are limited to the range with $z \geqslant d$.

For elastic indentation at each asperity, we can write $f(\delta) = f_0\delta$ and $g(\delta) = g_0\delta^{3/2}$, with f_0 and g_0 independent of δ [7]. Assuming for now that the surface is isotropic, so that the distribution of α is uniform with $\zeta(\alpha) = 1/2\pi$, so that θ' is distributed symmetrically about zero, we find that the contributions to N from the friction forces $\mathcal{F}$ at each asperity cancel, so that

$$N = \int_d^\infty g_0(z-d)^{3/2}\cos^{5/2}\theta\,\phi(z)\psi(\theta)\zeta(\alpha)\,dz\,d\theta\,d\alpha \tag{10}$$

and similarly for the total horizontal force

$$F = \int_d^\infty sf_0(z-d)\cos\theta\cos\theta'\,\phi(z)\psi(\theta)\zeta(\alpha)\,dz\,d\theta\,d\alpha. \tag{11}$$

These cancellations arise since for every contact with a given indentation and angle θ' in a large ensemble of spherical asperities, there is likely to be another with the opposite value of θ'.

Equations (10) and (11) lead to an effective friction coefficient equal to

$$\mu = \frac{F}{N} = \mu_0 \frac{\int \cos\theta\cos\theta'\,\psi(\theta)\zeta(\alpha)\,d\theta\,d\alpha}{\int \cos^{5/2}\theta\,\psi(\theta)\,d\theta} \tag{12}$$

where μ_0 is, as before, the friction coefficient ignoring the inclination of contacts. Now, for small angles θ and θ' we have

$$\cos\theta' \approx 1 - \tfrac{1}{2}\cos^2\alpha\tan^2\theta \tag{13}$$

so that the integral over α in equation (12) may be performed with $\zeta(\alpha) = 1/2\pi$, giving

$$\mu = \mu_0 \frac{\int \cos\theta(1 - \frac{1}{4}\tan^2\theta)\,\psi(\theta)\,d\theta}{\int \cos^{5/2}\theta\,\psi(\theta)\,d\theta}. \tag{14}$$

By expanding the integrands the friction coefficient for elastic indentation may therefore be written

$$\mu = \mu_0(1 + \tfrac{1}{2}\langle\theta^2\rangle) \tag{15}$$

for small angles θ, where the angled brackets denote the mean value over the distribution $\psi(\theta)$.

This result is less dependent on roughness than expected from the one-asperity analysis. The Tabor analysis can only be applied to the present case by allowing a narrow slider to pass over the rough surface, always taking the steepest path up and down the asperities. The apparent friction coefficient fluctuates as the slider moves, but an average can be calculated. From equation (4), the friction coefficient in these circumstances would be $\mu_0(1 + \langle\theta^2\rangle)$ for small angles and small μ_0.

The θ dependence is less when the surface is taken to respond plastically to the indentation. With $f(\delta) = f_0'\delta$ and $g(\delta) = g_0'\delta$, where f_0' and g_0' are new coefficients describing plastic indentation [7], the expression for μ equivalent to equation (14) is

$$\mu = \mu_0 \frac{\int \cos\theta(1 - \frac{1}{4}\tan^2\theta)\,\psi(\theta)\,d\theta}{\int \cos^2\theta\,\psi(\theta)\,d\theta} \tag{16}$$

and so

$$\mu = \mu_0(1 + \tfrac{1}{4}\langle\theta^2\rangle) \tag{17}$$

for plastic deformation.

These results have been derived using an extended Greenwood–Williamson model, which restricts asperity peaks to being spherical with constant curvature. An extension to more general surface properties is made in the next section using numerical contact simulation.

3. Numerical calculations

The basis of the calculations made here is a numerical contact model developed by Ogilvy [8]. Modifications to the original code have been made to consider the contact of two random rough surfaces rather than a rough surface and a rigid flat, and to calculate the orientation of the local normal at each contact point. The code has also been changed to use the analysis of forces at each asperity described above and illustrated in figure 3. We do not allow asperities to move around each other as the surfaces slide.

The simulation proceeds by generating two surfaces numerically with the required statistical properties [8]. The distribution of heights above a mean plane is Gaussian with a specified RMS roughness. Correlation lengths in the x and y directions in the two-dimensional plane characterize the rate of change of height along the surface. The effective rough surface is then brought into contact with a rigid flat, until the total reaction force balances the applied load. The apparent indentation at each contact is adjusted according to the inclination angle, noted from the original surface geometry, in the same fashion as described in equation (5). Several realizations of the surfaces are generated, each of which is used to determine a friction coefficient, given by the total force in a specified horizontal direction divided by the total vertical force.

In general, the friction coefficient for a realization will depend on the direction of sliding. Furthermore, it can be negative, if most contacts are descending and the inclination angles are large enough. In order to reduce the spread of results, each surface realization was analysed twice: once for sliding forwards and once for sliding backwards along a specified direction. This corresponds to incrementing the angle α at each contact by π, and repeating the analysis. The friction coefficients in each case were averaged and the mean and variance of this averaged quantity estimated from the ensemble.

The same ensemble of realizations is used to study surfaces of different roughnesses, by simply scaling the heights. This introduces correlations in the mean friction coefficients at each roughness, as we discuss below.

Example calculations were performed for sliding between two surfaces generated with the same statistical properties. Material properties that are representative of diamond were used, though the applicability of the model to this system is debatable, since the model assumes that the underlying friction mechanism is adhesion between the surfaces at each contact, and ignores other mechanisms such as cracking. The mechanism of friction in diamond is discussed further in [3, 9, 10]. The material properties of diamond are reviewed in [11] and those chosen for use here are given in table 1.

Diamond is usually considered to be an ideally brittle material and unable to deform plastically. However, it has been suggested that plastic flow does occur in diamond at room temperature, especially under indentation loading conditions [12], and that it plays a role in room-temperature friction of diamond on diamond [10]. The yield stress given in table 1 is the tensile fracture stress measured in indentation tests [11] but is used here for illustration.

Table 1. Material properties representative of diamond for the numerical contact model. The data are reviewed in [11]. The yield stress given is actually the failure stress in tension. Possible alteration of the properties due to the thin film nature is ignored.

Property	Value	Reference
Young's modulus	1050 GPa	[14]
Poisson's ratio	0.2	[14]
Yield strength	3 GPa	[11]
Surface shear strength	0.33 GPa	[11, 13]

First, a purely elastic calculation was performed, by disabling the usual plastic deformation model in the code. Figure 4 shows how the friction coefficient depends on the roughness of the real surfaces calculated from 75 realizations with area 36 μm^2. The correlation lengths in the x and y directions on the surface were 0.125 μm, chosen to produce appreciable inclination angles for the range of roughnesses considered. A typical asperity has a width of a few correlation lengths. The number of contact points falls from about 90 at the lowest roughness to about six at the highest. The friction coefficients tend to fall with increasing roughness, due to decreasing real contact area for a given load. This was noted in [8].

The curve in figure 4 represents results when one surface is taken to be perfectly flat, so that all inclination angles at the contacts are zero. These are denoted smooth slider results. The circles correspond to both surfaces being rough, and these are labelled rough slider results. The latter are plotted against a combined RMS roughness R_c:

$$R_c^2 = R_1^2 + R_2^2 \tag{18}$$

where $R_{1,2}$ are the RMS roughnesses of the two surfaces. Since $R_1 = R_2$, $R_c = \sqrt{2}R_1$. The mean friction coefficients for the rough slider exceed those for the smooth slider, with the difference increasing with roughness. The standard deviation in each friction coefficient is not shown: a typical statistical error is 25% for the roughest surfaces and about 10% for the smoothest. In spite of these variations, the mean values lie along a reasonably smooth curve due to the use of scaled versions of each numerically generated surface to represent different roughnesses. For this reason, the enhancement factor due to the rough slider contact is visible in the numerical results in spite of statistical fluctuations of the same order of magnitude.

The RMS contact angle $\langle\theta^2\rangle^{1/2}$ at the asperities for the two rough surfaces is calculated numerically and is also shown in figure 4. This value is inserted into equation (15) to obtain a theoretical correction factor by which the rough slider and smooth slider results should differ, according to the previous analytical development. The crosses in figure 4 show the rough slider results reduced

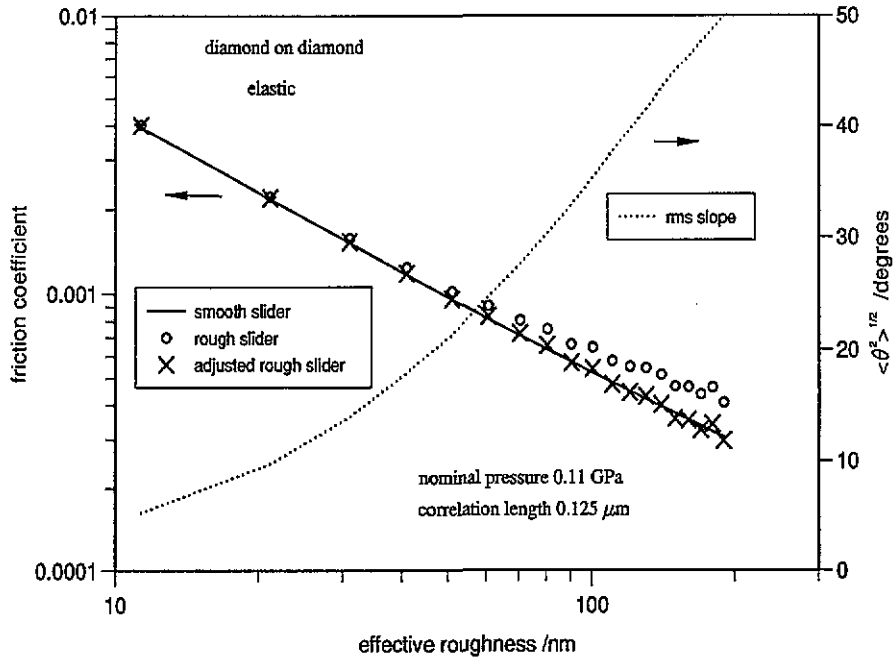

Figure 4. Friction coefficient against effective roughness for contact between a rough surface and either a smooth slider (curve) or a rough slider (circles). The rough slider results are adjusted according to the expected enhancement factor and plotted as crosses for comparison with the smooth slider results.

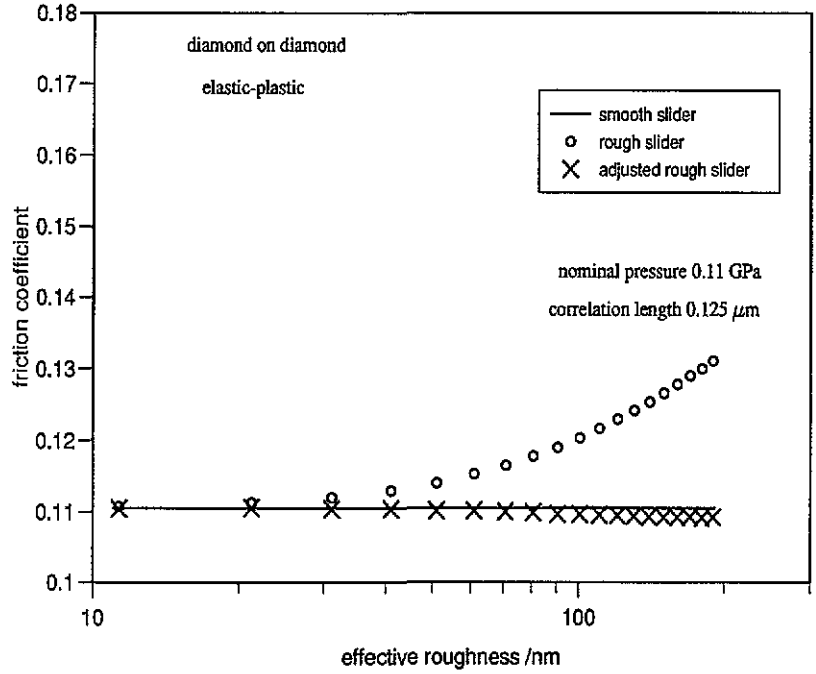

Figure 5. Friction coefficient against effective roughness for contact between a rough surface and either a smooth slider (curve) or a rough slider (circles). This case takes into account both plastic and elastic deformation.

by this factor. Although the comparison is affected a little by statistical fluctuations at high roughnesses, it is clear that the differences between rough and smooth slider friction coefficients are consistent with the predictions of the model.

An elastoplastic calculation underlines the above conclusions. The same loading conditions were used as in the elastic calculation, but with the plastic model operating: the deformation of the asperities was then almost entirely plastic. Only 25 realizations were

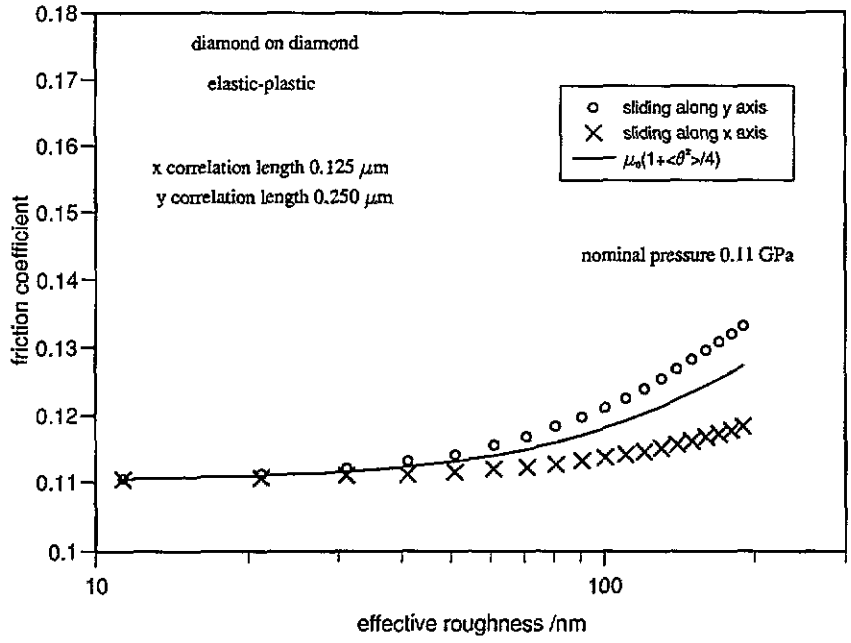

Figure 6. Friction coefficient against effective roughness for contact between rough surfaces with elongated asperities, which tend to be aligned with the elongation along the y axis. The friction coefficient is greater for sliding in the y direction than it is for the x direction.

generated and analysed for this case. Figure 5 compares the mean friction coefficient against effective roughness for a rough slider (circles) and a smooth slider (curve). Errors in the mean friction coefficients are small in these calculations (about 2%) since, when deformation is largely plastic, the mean pressure at each asperity tends to a constant, as noted in [8]. This effect also reduces the dependence of μ on the roughness, compared with the purely elastic case. Once again, the results for the rough slider lie above those for the smooth slider, for the same effective roughness. To test the validity of equation (17), the rough results are reduced by the expected enhancement factor, using values of $\langle\theta^2\rangle$ generated from the simulation. These adjusted rough results are shown as crosses, and since they lie close to the smooth slider results we conclude that equation (17) provides a good description of the roughness effect for elastoplastic contact, for this range of contact angles. This is in spite of the fact that in the simulation the asperities are not spherical and possess a range of curvatures.

The numerical code allows more complex cases to be considered, beyond the assumptions of the Greenwood–Williamson model. In particular, it is of interest to calculate the direction dependence of the friction coefficient, for non-isotropic surfaces. Figure 6 shows the friction coefficient against effective roughness for contact between surfaces both having a correlation length in the y direction twice that in the x direction, 0.250 and 0.125 μm respectively. The asperities are therefore typically elongated in the y direction. Two cases are shown, each based on 20 realizations, with relative motion of the surfaces along the x axis and the y axis, respectively. Unexpectedly, it is found that the friction coefficient in the y direction is greater than that in the x direction, even though it is for the latter that values of θ', the angle of ascent at the contacts, resolved in the sliding direction, are greater. The results can, however, be understood using equations (8) and (9), and a revised distribution of angles α. If sliding is in the direction of the long axis of the asperities, then α is not uniformly distributed, but instead values clustered around $\pm\pi/2$ are favoured. In this limit we have $\theta' \approx 0$, and so for plastic indentation the development leads to $\mu = \mu_0(1 + \frac{1}{2}\langle\theta^2\rangle)$. The roughness effect is twice that for an isotropic surface. In the opposite extreme, where motion is along the short axis of the asperities, $\alpha \approx 0$ or π and $\theta' \approx \pm\theta$, so the model suggests $\mu = \mu_0$, independent of roughness, again for plastic deformation. The two situations studied numerically should provide friction coefficients somewhere between the isotropic prediction, shown as a curve in figure 6, and the two extreme cases just considered. This is indeed the case, as figure 6 indicates. The model predicts that similar effects would arise for elastic indentation.

4. Discussion and conclusions

This paper has developed the ideas suggested by Tabor [3] concerning the influence of surface roughness on friction. The original analysis treated the passage of a single contact point over an asperity on the opposing surface. More realistic friction problems, however, involve multi-asperity contact between rough surfaces, with a range of asperity curvatures, heights and, in particular, the angle of inclination θ between the local normal at the contact point and the overall normal. We have extended the Greenwood–Williamson model of

rough surface contact to take into account variations in θ. The local reaction and friction forces at each contact are resolved in the sliding and overall normal directions, and related to the mean separation between the contacting planes. By summing the total forces, an effective friction coefficient can be obtained.

The effect of the contact angle distribution has been investigated analytically for pure elastic and pure plastic indentation. This approach leads to an effect less than that suggested by the Tabor analysis: the reason is that cancellation occurs when the total forces are calculated, since there are many asperity contacts instead of just one. Furthermore, the effect depends on the mode of deformation. For elastic contact, the additional contribution to the friction coefficient increases with roughness, but is about half that expected. For plastic contact, the contact angle effect is about one quarter of the Tabor result.

These conclusions have been illustrated using a numerical simulation of elastic and elasto-plastic contact between rough diamond surfaces, based on a code due to Ogilvy [8]. The asperities are no longer taken to be spherical and of equal curvature, which is assumed in the Greenwood–Williamson model, but the results are consistent with the analytical predictions. A previous numerical study of the contact between rough surfaces allowing for non-zero inclination angles at the contacts showed similar agreement with the Greenwood–Williamson model, though no attempt was made to study friction [15].

The numerical code has been used to study the directional dependence of the friction coefficient for anisotropic surfaces, where the asperities tend to be elongated in a particular direction. It has been demonstrated that the friction coefficient is larger for sliding in the direction of asperity elongation than in the direction perpendicular to this. Such a conclusion is counter-intuitive, and it would be interesting to find experimental confirmation.

Our main objective has been to demonstrate the effect of contact angle on the friction coefficient. However, the loading parameters for the numerical calculations have been chosen to be similar to those used experimentally by Hayward *et al* [6] in a study of friction between diamond films. We have also used a correlation length of 0.125 μm in order to obtain large contact angles, approaching those described in [6]. Experimentally, friction coefficients increased with roughness from about 0.03 to 0.4 within the same range of roughnesses studied here [6]. It would appear from figure 4 that the calculations assuming elastic deformation at the asperities show a steep decrease in friction coefficient with increasing roughness, which is not reversed by the roughness effect developed in this paper. Increasing the correlation length can increase the friction coefficient for the elastic case to more reasonable values [8], but this does not improve the roughness dependence.

An assumption of plastic deformation at the asperities, however, produces friction coefficients of the correct order of magnitude with a qualitatively correct roughness dependence, as shown in figure 5. It is, however, questionable whether diamond surfaces are capable of significant plastic deformation. Further consideration of the data in [6] will require a clarification of the deformation and fracture response of diamond films under high loads.

Acknowledgments

This work was funded by the Corporate Research programme of AEA Technology. I thank Dr J A Ogilvy for instruction in the use of her numerical contact model. I also thank Dr J A Greenwood for some important contributions.

References

[1] Coulomb C A 1785 *Mémoires de Mathématique et de Physique de l'Academie Royale des Sciences* (Paris: Academie Royale des Sciences) p 161
[2] Leslie J 1804 *An Experimental Inquiry into the Nature and Propagation of Heat* printed for J Newman, No 22, Poultry (T Gillet Printer, Salisbury Square)
[3] Tabor D 1979 *The Properties of Diamond* ed J E Field (London: Academic) ch 10
[4] Seal M 1981 The friction of diamond *Phil. Mag.* A **43** 587
[5] Greenwood J A and Williamson J P B 1966 Contact of nominally flat surfaces *Proc. R. Soc.* A **295** 300
[6] Hayward I P, Singer I L and Seitzman L E 1992 Effect of roughness on the friction of diamond on CVD diamond coatings *Wear* **157** 215
[7] Johnson K L 1985 *Contact Mechanics* (Cambridge: Cambridge University Press)
[8] Ogilvy J A 1992 Numerical simulation of elastic-plastic contact between anisotropic rough surfaces *J. Phys. D: Appl. Phys.* **25** 1798
[9] Samuels B and Wilks J 1988 The friction of diamond sliding on diamond *J. Mater. Sci.* **23** 2846
[10] Feng Z and Field J E 1991 Friction of diamond on diamond and chemical vapour deposition diamond coatings *Surf. Coatings Technol.* **47** 631
[11] Field J E (ed) 1979 *The Properties of Diamond* (London: Academic) ch 9
[12] Brookes C A and Brookes E J 1991 Diamond in perspective: a review of mechanical properties of natural diamond *Diamond Related Mater.* **1** 13
[13] Hull E H and Malloy G T 1966 *J. Eng. Ind.* **88** 373
[14] Grimsditch M H and Ramdas A K 1975 Brillouin scattering in diamond *Phys. Rev.* B **11** 3139
[15] McCool J I and Gassel S S 1981 The contact of two surfaces having anisotropic roughness geometry *ASLE Special Publication* **SP-7** (ASLE) p 29